Quantifying non-invasive MRI parameters with angiogenesis and cellular infiltration to characterize collagen-sponge remodeling

Mohammed Salman Shazeeb[1,2], Sivakumar Kandasamy[2], Stuart Howes[2], and George Pins[2]

[1]*Radiology, University of Massachusetts Medical School, Worcester, MA, United States,* [2]*Biomedical Engineering, Worcester Polytechnic Institute, Worcester, MA, United States*

Introduction: Current methods for evaluating the remodeling of soft biomaterial implants involve the surgical removal of the implant for subsequent histological assessment [1]. This approach is invasive, often destructive, and imposes practical limitations on how effectively these materials can be evaluated. MRI has the potential to non-invasively monitor the remodeling of collagen scaffolds, particularly the biodegradation, cellular infiltration, and extracellular matrix deposition within the scaffold [2-5]. In this study we continued to investigate the development of a non-invasive system to evaluate the angiogenic and cellular infiltration aspects associated with the remodeling of implanted collagen scaffolds using MRI and correlated the MRI measurements to conventional histological techniques.

Methods: Three types of sponges were fabricated using scaffolds prepared from insoluble bovine collagen as described in [6]: 1.) the first type was crosslinked with 1-ethyl-3-(3-dimethyl aminopropyl) carbodiimide (EDC) to increase resistance to biodegradation; 2.) the second type, chondroitin 6-sulphate (CS), was used with EDC (EDC+CS) to increase the biocompatibility of the sponge, and; 3.) the third type was hydrated in MES buffer only and designated as uncrosslinked (UNX). Each sponge type was implanted in dorsal subcutaneous pockets of Sprague-Dawley rats (n=8). Two days after surgery and then weekly for up to 6 weeks, MRI experiments were performed at 2.0T to image the sponges. T_2-weighted images were acquired with the following parameters: TR=2500ms, 12 echo times from TE=12–144ms, FOV=6cm×4cm, matrix=256×128, slice thickness=2mm, NEX=2. Diffusion-weighted imaging (DWI) was performed using a spin-echo, echo-planar imaging pulse sequence with diffusion-sensitive gradient pulses (b values=15–760 mm^2s^{-1}) applied along three different gradient axes with gradient separation Δ=35ms and gradient duration δ=4ms. Other parameters were: TR/TE=2000ms/53ms, matrix=64×64, slice thickness=2mm, NEX=2. T_2 maps and apparent diffusion coefficient (ADC) maps were generated from T_2- and DWI images. For contrast-enhanced MRI (CEMRI), a pre-contrast image was acquired using a T1-weighted, spin-echo pulse sequence (TR=600ms, TE=10ms, slice thickness=2mm, NEX=2). Gadolinium-DTPA (Gd-DTPA) was then administered intravenously via tail vein (0.1mmol/kg). Post-contrast images were acquired 5 mins post-injection and then at 10-min intervals up to 170–240 mins. The times required to attain the maximum signal intensity change and to decline to 50% of this peak value were measured as the Time-To-Peak (TTP) and $T_{1/2}$ (T-Half) Time, respectively. Animals were euthanized and sponges were harvested at each of the imaging time points to perform histology using Heamotoxylin & Eosin (H&E) and Masson's trichrome. The blood vessel density, cellular density, and void area fraction of each scaffold was quantified to determine angiogenesis, cellular infiltration, and overall tissue growth into the scaffolds, respectively.

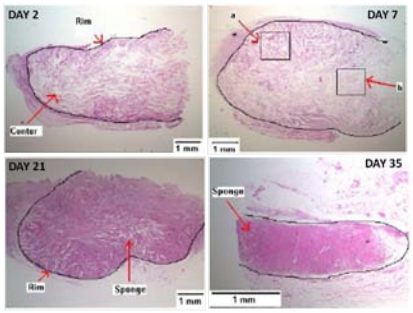

Fig. 1 – H&E histological section of EDC+CS (Days 2, 7, and 21) and EDC (Day 35) sponges shown at different days following implantation. (a) and (b) on Day 7 indicate regions of cellularity and porosity, respectively.

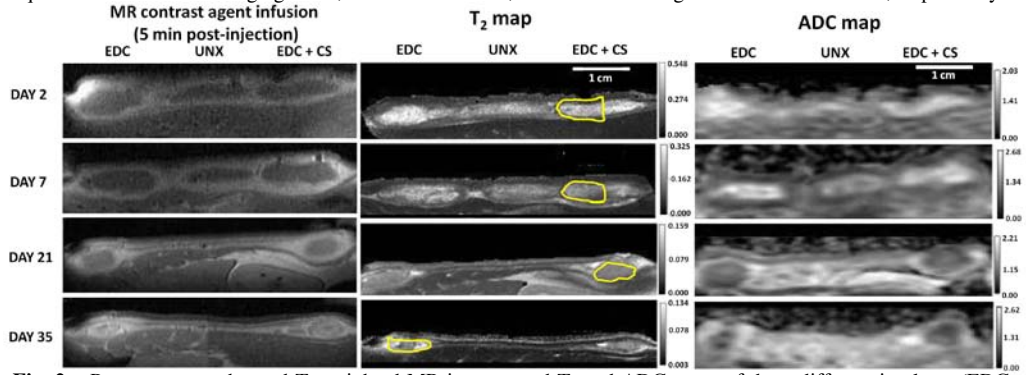

Fig. 2 – Post-contrast enhanced T_1-weighted MR images, and T_2 and ADC maps of three different implants (EDC, UNX, and EDC+CS) shown at different time points after implantation. T_2 map scale-bar values are in seconds and ADC map scale-bar values are ADC×10^{-5} cm^2/s. Yellow demarcations in T_2 map approximate the locations of histological sections shown in Fig. 1.

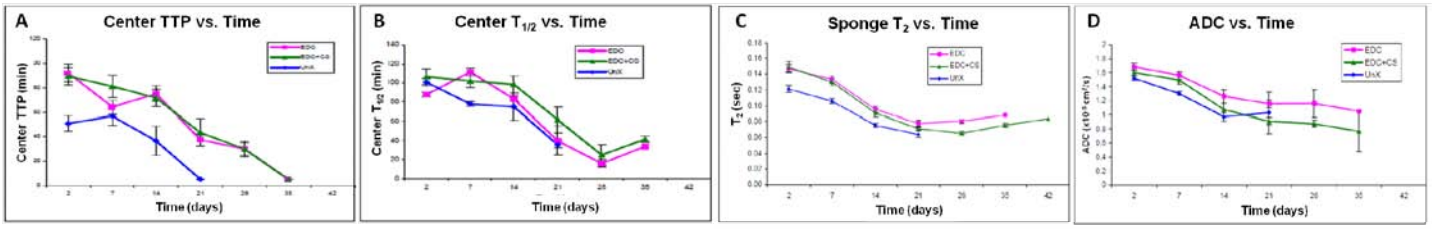

Fig. 3 – (**A**, **B**) Plots of time-to-peak (TTP) values and $T_{1/2}$-time values as a function of implantation time in the center regions of different sponge types. (**C**, **D**) Plots of T_2-relaxation times and water ADC values as a function of implantation time for different sponge types. Error bars represent SEM from all the animals analyzed.

Results and Discussion: The initial H&E section from the sponges showed lattice-like matrix appearing to form a highly porous interconnecting network with a rim comprised of a thin layer of infiltrated cells (Fig. 1). With time, the rim showed a higher degree of cellular infiltration and the center showed little remaining porous structure, which progressively became more homogeneous with complete cellular infiltration and integration with surrounding tissues. The calculated T_2 and ADC maps (Fig. 2) showed a reduction in the T_2 and ADC values with time (Fig. 3CD), which is consistent with an increase in cellular infiltration and tissue ingrowth. Significant differences between UNX and both cross-linked sponges at all time points ($p<0.01$) were observed, except at Day 21. UNX ADC values were significantly reduced compared to those of EDC sponges at time points <21 days ($p<0.03$). At 5-mins post-injection, CEMRI showed a thin line of rapid contrast enhancement in the sponge rim (Fig. 2); however, in the sponge center, contrast uptake and washout was significantly delayed. The TTP values showed a decreasing trend in the centers of all three sponge types with a significant difference between UNX and cross-linked sponges at Days 2 ($p<0.002$), 14 ($p<0.05$), and 21 ($p<0.03$) (Fig. 3A). Similar results were observed with changes in $T_{1/2}$-times at all time points (Fig. 3B) except Day 7 ($p<0.02$ between UNX and cross-linked sponges). The TTP and $T_{1/2}$ times reduced due to increased angiogenesis and reduction in sponge thickness with time. Calculations from histology showed an increasing trend in blood vessels (angiogenesis) and cell numbers (increased cellular infiltration), and a decreasing trend in the void fraction (increased tissue ingrowth) with increasing time for all scaffolds (data not shown).

Conclusion: The histological measurements corroborate the changes in CEMRI, and T_2 and ADC maps which reflect the *in vivo* remodeling of collagen sponges. Understanding this relationship will help detect changes within implants using MRI data alone, reducing the need for scaffold harvesting and destructive testing. Ultimately, these tools will significantly enhance our ability to design and assess the next generation of robust biomaterial scaffolds for tissue regeneration.

References: [1] Hong *et al*. (2006). Tissue Eng **12**:843-854; [2] Packer (1977). Phil Trans R Soc Lond **278**:59-87; [3] Shazeeb *et al*. (2013). Proc Intl Soc Mag Reson Med **21**:3085; [4] Viljanto *et al*. (1999). Wound Repair Regen **7**:119-126; [5] Kido *et al*. (2013). J Magn Reson Imag doi:10.1002/jmri.24282; [6] Pieper *et al*. (2000). Biomater **21**:1689-1699.